

RESEARCH ARTICLE | OCTOBER 02 2023

Effect of in-source beam shaping and laser beam oscillation on the electromechanical properties of Ni-plated steel joints for e-vehicle battery manufacturing ✓

Special Collection: [Proceedings of the International Congress of Applications of Lasers & Electro-Optics \(ICALEO 2023\)](#)

Leonardo Caprio  ; Barbara Previtali  ; Ali Gökhan Demir 



J. Laser Appl. 35, 042030 (2023)

<https://doi.org/10.2351/7.0001151>



View
Online



Export
Citation

[CrossMark](#)



RAPID TIME
TO ACCEPTANCE



COMMUNITY
DRIVEN



EXPANSIVE
COVERAGE



PRESTIGIOUS
EDITORIAL BOARD



EXTENSIVE
MARKETING

Effect of in-source beam shaping and laser beam oscillation on the electromechanical properties of Ni-plated steel joints for e-vehicle battery manufacturing

Cite as: J. Laser Appl. 35, 042030 (2023); doi: 10.2351/7.0001151

Submitted: 3 July 2023 · Accepted: 11 September 2023 ·

Published Online: 2 October 2023



Leonardo Caprio,^{a)} Barbara Previtali, and Ali Gökhan Demir

AFFILIATIONS

Department of Mechanical Engineering, Politecnico di Milano, Via Giuseppe La Masa 1, Milano 20156, Italy

Note: Paper published as part of the special topic on Proceedings of the International Congress of Applications of Lasers & Electro-Optics 2023.

^{a)}Author to whom correspondence should be addressed; electronic mail: leonardo.caprio@polimi.it

ABSTRACT

Laser welding is a key enabling technology that transitions toward electric mobility, producing joints with elevated electrical and mechanical properties. In the production of battery packs, cells to busbar connections are challenging due to strict tolerances and zero-fault policy. Hence, it is of great interest to investigate how beam shaping techniques may be exploited to enhance the electromechanical properties as well as to improve material processability. Industrial laser systems often provide the possibility to oscillate dynamically the beam or redistribute the power in multicore fibers. Although contemporary equipment enables elevated flexibility in terms of power redistribution, further studies are required to indicate the most adequate solution for the production of high performance batteries. Within the present investigation, both in-source beam shaping and beam oscillation techniques have been exploited to perform 0.2–0.2 mm Ni-plated steel welds in lap joint configuration, representative of typical cell to busbar connections. An experimental campaign allowed us to define process feasibility conditions where partial penetration welds could be achieved by means of in-source beam shaping. Hence, beam oscillation was explored to perform the connections. In the subset of feasible conditions, the mechanical strength was determined via tensile tests alongside electrical resistance measurements. Linear welds with a Gaussian beam profile enabled joints with the highest productivity at constant electromechanical properties. Spatter formation due to keyhole instabilities could be avoided by redistributing the emission power via multicore fibers, while dynamic oscillation did not provide significant benefits.

Key words: laser welding, beam shaping, electric mobility, battery manufacturing

Published under an exclusive license by Laser Institute of America. <https://doi.org/10.2351/7.0001151>

I. INTRODUCTION

The electric mobility sector is focusing on the development of highly efficient battery systems to provide competitive solutions with respect to internal combustion engines. In order to obtain the desired voltage, capacity, and current rating of battery packs, multiple cells need to be connected in series and parallel, and different joining technologies may be employed.^{1–3} Currently, Li-based batteries are the reference solution for the realization of high performance battery packs.⁴ Li-based batteries are typically realized in

different form factors (namely, cylindrical, pouch, and prismatic cells).⁵ Different joining solutions have been explored throughout the scientific and industrial communities for the realization of cell to busbar connections in order to manufacture operational battery packs. The selection of the technological process often relies on a compromise between the applicability, performance, capital cost, and productivity of the available solutions for a specific geometry. For instance, ultrasonic welding processes may be exploited for the joining of pouch or prismatic cells but are less apt for the joining of cylindrical cells.⁶ Analogously bolted connections may be

17 October 2023 07:26:27

applicable for connecting prismatic cell connectors,⁷ while they result in excessive incumbrance for the realization of battery packs composed of multiple cylindrical cells.⁸

The present investigation focuses on evaluating novel beam shaping solutions for the laser of Li-ion cylindrical cells. The connection between these cells is typically performed by either resistance spot welding (RSW) or laser welding. RSW has become a popular solution given its simple applicability and low cost.^{9,10} Moreover, it possesses the significant advantage of ensuring the absence of a gap between the welding electrodes and the two sheets being contacted, given the intrinsic necessity of applying pressure to perform the joining operation. On the other hand, the noncontact nature of the laser welding process provides the advantage of higher productivity while avoiding tool wear. Laser welding is becoming the reference technique for the production of battery packs with Li-ion cylindrical cells. For instance, Brand *et al.* demonstrated that laser welding can realize connections with the highest performance in terms of mechanical and electrical properties for CuZn37 busbar connections to 26 650 Li-ion cells.¹¹

Concurrently, the state-of-the-art laser welding systems propose innovative solutions that can be appealing process solutions, although demonstrative studies are required to disclose their actual impact. For instance, novel generation laser sources emitting in the blue and green wavelengths are promising for the realization of laser welded connections of thin sheet materials highly reflective to conventional near-infrared laser radiation.^{12,13}

Within the industrial and scientific communities, there is a strong interest toward the use of beam shaping techniques to modify the power spatial distribution. In particular, two of the most commonly examined approaches are dynamic oscillation of the laser beam and in-source beam shaping via the use of multicore fibers. Dynamic beam oscillation relies on high frequency motion of the laser beam superimposed to the translation direction of the weld trajectory. In-source beam shaping may be achieved within the laser source by allocating the laser emission to different transport fibers positioned coaxially such that the spatial emission profile corresponds to the superposition of a Gaussian beam (transported in the inner core) and ring mode (via the outer core). For instance, Schmidt *et al.* provided a comprehensive analysis regarding laser welding of Al/Cu in lap joint configuration, indicating that dynamic beam oscillation can help us to enlarge the weld seam, thus reducing the electrical resistance.¹⁴ Punzel *et al.* exploited multicore fiber to reduce porosity formation during the welding of different Al-alloys.¹⁵ Prieto *et al.* and Sun *et al.* also investigated the tailoring of the power distribution for the welding of Al for e-mobility applications.^{16,17} Chianese *et al.* explored beam oscillation for the joining of copper to steel joints, while Rinne *et al.* exploited in-source beam shaping.^{18,19}

Even though there has been significant attention toward the use of such techniques, a comprehensive study is required to understand the effects over the electrical characteristics of laser welded joints. Often, research has been focused on the enabling aspects of beam shaping solutions, while open questions remain with regard to which approach is more convenient in terms of the electromechanical properties of the joints.

The redistribution of the emission power with the use of dynamic beam oscillation or the use of multicore fibers may allow us to achieve joints with a larger seam width, possibly suppressing

the spatter formation and allowing for a more tolerant process in terms of penetration depth. There is evidence within the scientific literature that beam shaping techniques may improve the mechanical and electrical properties of the joints. For instance, Schmidt *et al.* demonstrated an inversely proportional correlation between the connection area (represented by the interface width) and the electrical resistance of Al/Al, Al/Cu, and Cu/Cu joints.¹⁴ With regard to the resistance of the Al/Al lap joint, Sun *et al.* showed that an increase in the amplitude of the laser beam oscillation yields an increase in the interface width, which is directly proportional to the weld strength.²⁰ Hence, it can be expected that the use of beam shaping techniques may be exploited to tailor the weld geometry in order to improve the electromechanical properties of joints.

Specifically, for e-mobility applications, the combined use of in-source beam shaping with dynamic beam oscillation has not yet been assessed. Hence, the aim of the current investigation is to disclose the effect of in-source and dynamic beam oscillation over the electromechanical properties for the welding of thin Ni-plated steel sheets in lap-joint configuration. This joint configuration simulates a typical solution employed to connect Li-ion cylindrical cells and a busbar and requires a partial penetration connection to avoid electrolyte expulsion. A flexible welding system with a multicore fiber laser enabling both in-source and dynamic beam shaping was employed to explore the process feasibility window with both techniques. Having defined stable processing conditions, a second part of the study focused on the definition of the electrical resistance of the connections as well its mechanical strength, comparing the novel solutions with conventional resistance spot welded (RSW) connections.

II. MATERIALS AND METHOD

A. Material and joint geometry

The scope of the present work consisted in determining the mechanical and electrical properties of cell to busbar connections and exploiting novel solutions for the laser welding process. For such reasons, the welding of two Ni-plated steel sheets of 0.2 mm thickness in lap joint configuration was performed with different welding systems, where the lower sheet simulated the cell casing while the upper material represented the sheet typically employed to connect in series and parallel the different cells. The material employed for the current investigation was a 0.2 mm thick Ni-plated steel sheet specifically designed for the realization of cell casings and connectors (Hilumin, Tata Steel Europe, London, United Kingdom).

B. Welding systems

A remote fiber laser welding system enabled both in-source and dynamic beam shaping of the laser emission. The system was composed of a laser source, which could redistribute the emission power between an inner core and an outer core of the transport fiber (nLIGHT, AFX1000, Vancouver, Washington, USA). The main specifications of the laser welding setup are reported in Table I.

17 October 2023 07:26:27

TABLE I. Main specifications of the laser welding system.

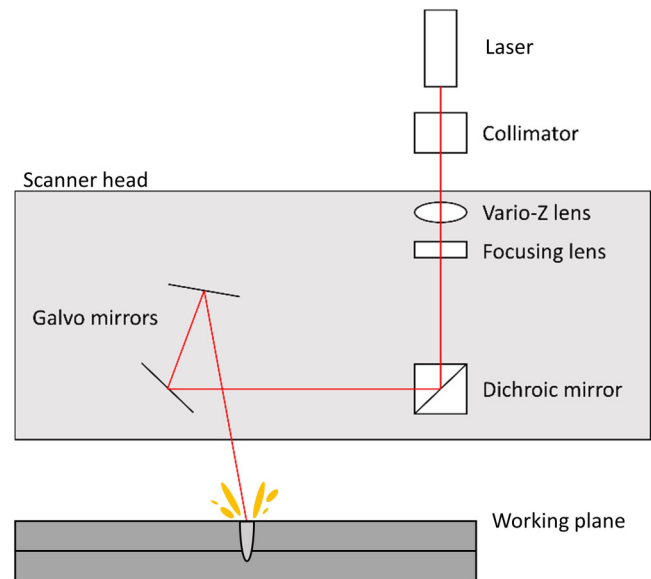
Parameter	Value
Emission wavelength, λ	1070 nm
Focal length of collimator, f_{col}	60 mm
Inner fiber core diameter, $d_{core,inner}$	14 μ m
External fiber core diameter, $d_{core,ext}$	40 μ m
Maximum power inner core, $P_{max,inner}$	600 W
Maximum power outer core, $P_{max,outer}$	1200 W
BPP inner beam, BPP_{inner} (mm mrad)	0.48
BPP outer beam, BPP_{outer} (mm mrad)	2.19
Beam waist diameter with BS0, $d_{0,BS0}$	70 μ m
Beam waist diameter with BS6, $d_{0,BS6}$	200 μ m

The inner core of the laser system corresponded to 14 μ m, while the outer core to 40 μ m. The inner core could transport up to 600 W of laser emission power, whereas the outer core could exploit the maximum emission power of the laser source corresponding to 1200 W. The laser beam exiting the transport fiber exhibited a beam parameter product of 0.41 mm mrad, whereas the BPP of the beam emitted from the outer core corresponded to 2.10 mm mrad. The process light was launched into a scanner head (AM module, Raylase, Wessling, Germany) via a collimating unit with a focal length of 60 mm.

Prior to the deflection by means of two galvanometric mirrors, the laser light was focused by two optical elements consisting in a fixed focusing lens and a fast moving lens in the Z direction, which allowed to compensate the focal position throughout the working plane. In the central position of the working field, theoretical calculations allowed us to estimate the beam waist diameter emitted from the inner single mode core at 70 μ m. In this case, the laser light was emitted from the outer core; the beam waist diameter was calculated at 200 μ m. The light propagation path is reported schematically in Fig. 1.

The laser emission power could be flexibly redistributed between the inner and outer core of the transport fiber. In order to indicate synthetically the power ratio distribution between the inner and outer core, the terminology beam shape BS_i has been introduced. The subscript i indicates a ratio in the distribution of the laser power from the inner toward the outer core. The corresponding power distribution between the inner and outer core of the transport fiber for the various BS are reported in Fig. 2. For instance, BS2 corresponds to 60% of the total emission power delivered to the inner core, whereas 40% is instead delivered via the outer core. Moreover, Fig. 2 shows the measurements of the spatial distribution of the emission power. The emission profiles were obtained by sampling the beam and exposing a CMOS camera sensor of a beam profiler (Gentec Beamage Series USB 3.0, Quebec City, Canada) according to procedures described in a previous publication.²¹

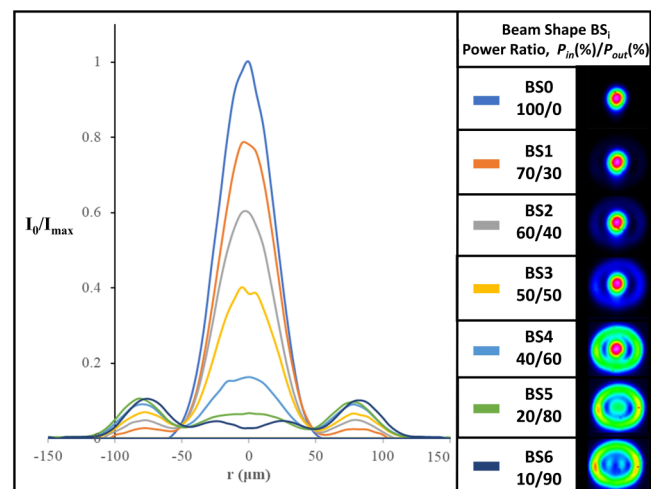
In order to compare the performance of laser welded joints with conventional joining techniques, a RSW machine was employed, namely, Glitter 801D (Joyfay Int, Cleveland, USA). The energy grade of the spot welding process could be regulated via its electronic control system.

**FIG. 1.** Schematic representation of the optical propagation path of the laser beam with the principal optical components of the remote welding system.

C. Characterization

Specimen geometry was defined in accordance with the standard ISO 14274:2016 for tensile testing and was maintained constant throughout the experimental activities. The weld region was maintained at the center of the specimen, while the other geometrical parameters are indicated in Fig. 3(a). The same specimen geometry could be employed for the characterization of the electrical

17 October 2023 07:26:27

**FIG. 2.** Spatial distribution of the emission power for the different beam shape indexes at different levels between the inner and outer core. The irradiance levels are reported with respect to the peak irradiance value.

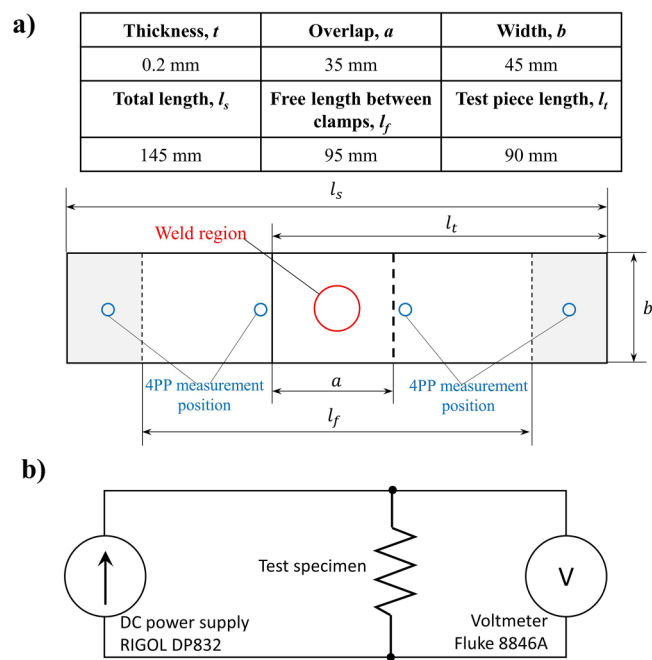


FIG. 3. (a) Specimen geometry and specifications and (b) 4 point-probe (4PP) connection scheme for the measurement of the electrical resistance.

resistance of the joint. Tensile testing was conducted on a universal testing machine (Alliance RT 100, MTS, Eden Prairie, MN, USA) with 100 kN maximum force allowing us to determine the ultimate tensile force (UTF).

Nondestructive electrical testing was conducted by imposing a fixed value of current of 3 A at the extremity of the samples by means of a calibrated DC power supply (DP832, RIGOL, Beijing, China). The voltage difference was then sampled by means of a high resolution nanovoltmeter (8846A, Fluke, Everett, WA, USA). An internal calibration procedure was developed and allowed us to estimate the measurement accuracy $0.4 \mu\Omega$. The connection scheme of the electrical measurement is shown in Fig. 3(b), while the connection positions are indicated in Fig. 3(a).

Standard metallographic analyses were employed to disclose the melt region generated by the welding process. Procedures consisted in cutting the weld transversally to the advancement direction, encapsulating the samples in resin followed by mechanical grinding and polishing of the metal surface. Chemical etching with a 5% Nital solution allowed us to observe the melt region that was acquired by means of an optical microscope (UM 300 I BD, EchoLAB, Paderno Dugnano, Italy). It was thus possible to measure the interface width of the joints, which corresponds to the width of the weld seam at the interface between the two sheets.

D. Experimental design to assess process feasibility

An experimental investigation was planned to determine the process feasibility by exploiting in-source and dynamic

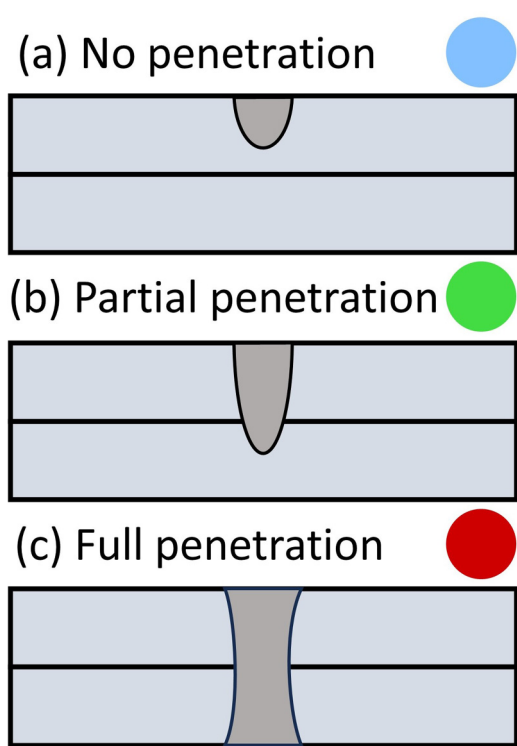


FIG. 4. Schematic representation of the categorical characterization of the process outcome.

beam shaping solutions enabled by the laser welding system. A first qualitative assessment of the process was conducted by observing the cross-sectional metallographies of the weld seam, allowing us to determine processability regions for the realization of successful cell to busbar connections. The weld seam could thus be classified into the following three categories [shown schematically in Fig. 4]:

- No penetration: The weld seam does not penetrate the underlying sheet. This condition is undesirable due to the fact that the connection between the busbar and cell is not generated.

TABLE II. Fixed and variable factors of the experimental design to assess the process feasibility of linear welds with in-source beam shaping.

Fixed factors	
Focal position, Δf (mm)	0
Trajectory	No oscillation
Variable factors	
Laser power, P (W)	300; 450; 600; 750; 900; 1050; 1200
Speed, v (mm/s)	100; 200; 300; 400; 500
Beam shape	BS0; BS2; BS4; BS6

17 October 2023 07:26:27

TABLE III. Fixed and variable factors of the experimental design to assess the process feasibility conditions of linear welds with in-source beam shaping and wobbling.

Fixed factors	
Focal position, Δf (mm)	0
Trajectory	Circular wobble
Wobble frequency, WF (Hz)	1000
Variable factors	
Laser power, P (W)	300; 600; 900; 1200
Speed, v (mm/s)	100; 200
Beam shape	BS0; BS2; BS4; BS6
Wobble amplitude, WA (mm)	0.2; 0.3

- Partial penetration: When the weld seam penetrates the first sheet completely and only partially the second underlying sheet hence corresponding to a successful connection
- Full penetration: When the weld seam completely melts both the top and bottom sheet. This output is undesirable since it implies that the laser beam can interact with internal parts of the cell.

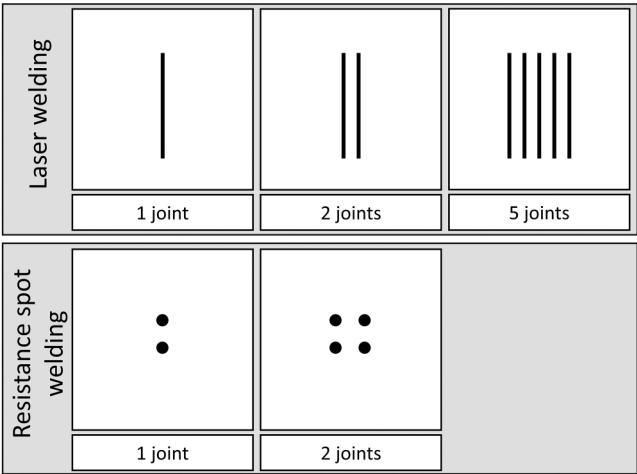


FIG. 5. Layout of the joint geometry for the comparison of the electromechanical properties.

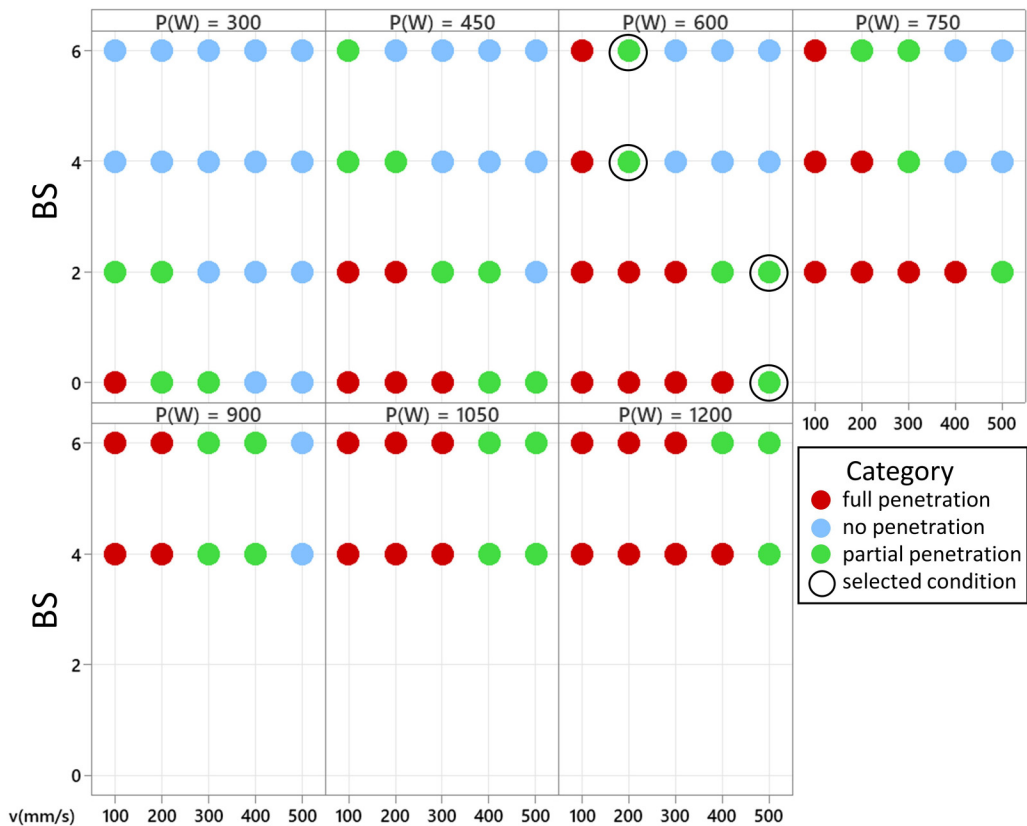


FIG. 6. Process feasibility map for the lap welding of Ni-plated steel exploiting different in-source beam shaping profiles.

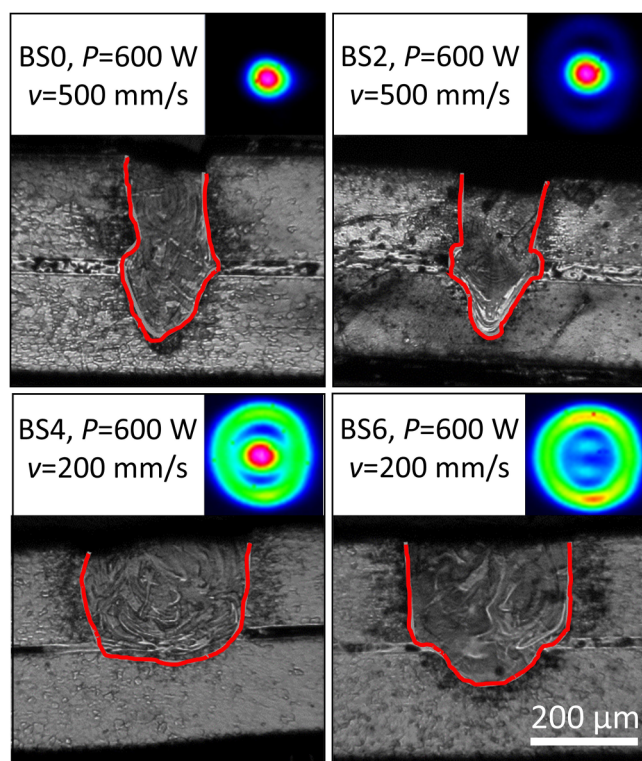


FIG. 7. Metallographic cross sections of the selected conditions when using in-source beam shaping. Red line indicates melt profile.

The joint geometry and specimen design were maintained constant throughout the investigation as previously presented. The connection consisted in a lap joint welding of two Ni-plated steel sheets with a straight linear weld trajectory with a length of 20 mm representative of connection paths.

An initial experimental campaign was designed with a wide range of process parameters to determine the process feasibility window with in-source beam shaping. Four of the beam shape indexes (namely, BS0, BS2, BS4, and BS6) were tested to investigate the effect of different spatial distributions over the process dynamics and outcome.

Laser power was varied between 300 and 1200 W with seven levels, depending on the applicability of the tested beam shape. Tests at power levels above 600 and 750 W could not be conducted with BS0 and BS2, respectively, due to power limitations on the inner core of the laser source. Five levels of weld speed from 100 to 500 mm/s were chosen. The fixed and variable factors of this design of experiments are reported in Table II.

A second experimental campaign was designed to assess the combined effect of wobbling and in-source beam shaping over the joint outcome. The results were analyzed categorically to determine the operational range with such solutions. A full factorial experimental campaign was designed (reported in Table III).

The welds were performed in a more restricted selection of laser powers from 300 to 1200 W with four levels and employing

the four beam shape distributions previously tested (BS0, BS2, BS4, and BS6). Two levels of weld speed ($v = 100; 200$ mm/s) and two levels of wobbling amplitude ($WA = 0.2; 0.3$ mm) were used. The wobbling frequency was maintained constant at 1000 Hz.

E. Experimental design for the characterization of the electromechanical properties

Having defined the feasible conditions for partial penetration joints exploiting both in-source and dynamic beam shaping, an experimental campaign was designed to study the electromechanical properties. Experiments were performed in the conditions selected in the previous phase and replicated five times. As an added point of comparison, iso-productivity conditions were also explored in this phase. Hence, beyond comparing the performance at a single joint level, by taking the less productive condition as a reference, multiple joints were performed with the higher productivity conditions until the productivity was matched. In practical terms, if two welding conditions employed weld speeds of v and $5v$, the number of weld joints were 5 and 1, respectively, to match the total welding time.

F. Comparison with RSW

In the final part of the experimental work, laser produced partially penetrating weld joint were compared to RSW welds using single and double joints. Figure 5 reports the schematical layout of different conditions tested. All the selected conditions were tested for their electrical resistance as well as their UTF.

III. RESULTS

A. Process feasibility with in-source beam shaping

Figure 6 shows the processability map at different levels of the emission power for the various processing conditions. It is possible to observe that at a fixed level of emission power, the Gaussian power distribution (BS0) allows us to perform partial penetration joints at higher scanning velocities with respect to the doughnut shape (BS6). This effect is expected to be correlated with the reduction of the peak irradiance, which is gradually reduced when redistributing the emission power from the inner toward the outer core. However, the use of higher levels of emission power with the doughnut beam shapes allows us to achieve comparable levels in terms of productivity.

The selection of the conditions was made at the highest level of power where all beam shapes were available ($P = 600$ W) where partial penetration joints could be achieved [indicated graphically by black circles in Fig. 6].

Representative metallographic cross sections of these conditions are shown in Fig. 7. Consistent with what may be expected, it is possible to observe that although similar penetration depths could be achieved, higher order beam shapes enabled a larger joint geometry.

The weld bead shape obtained in such conditions exhibits a regular profile, which is symptomatic of a more stable molten pool during the welding process, while BS0 and BS2 exhibit narrow deep penetration weld geometry. Exploiting the outer ring of the fiber, it was thus possible to regulate the aspect ratio of the joint geometry. Given the wide experimental design with single replicates, it is

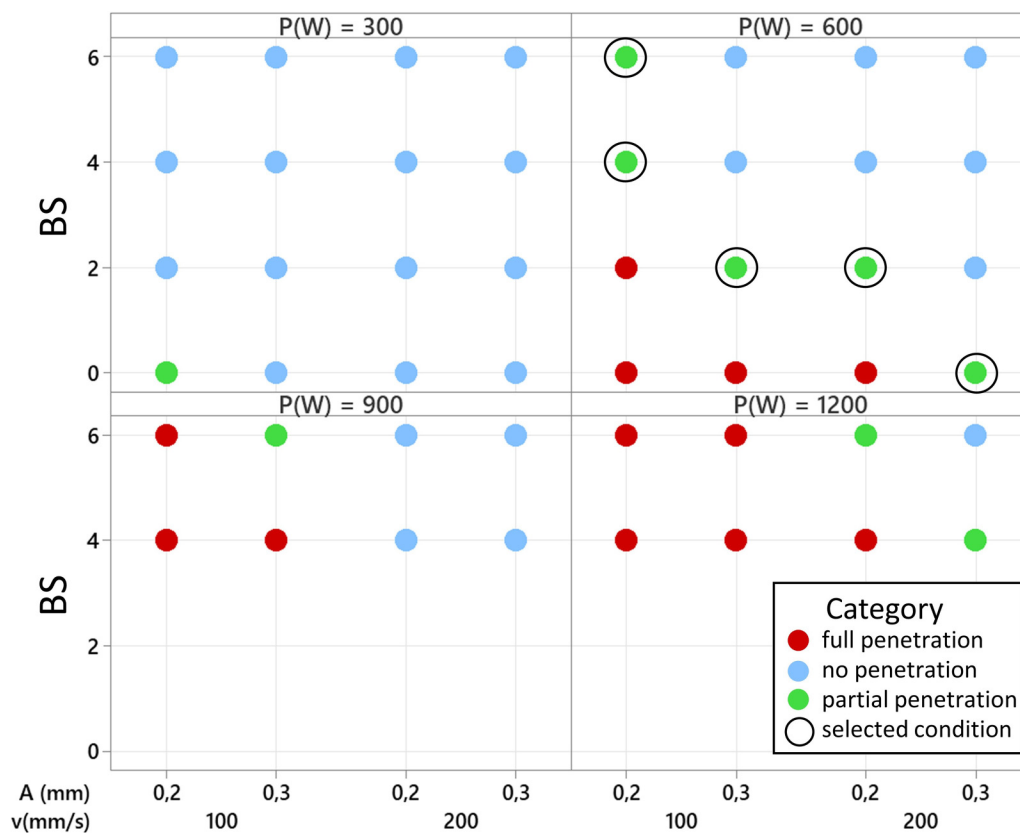


FIG. 8. Process feasibility map for the lap welding of nickel plated steel with the use of dynamic beam oscillation combined with in-source beam shaping.

difficult to draw conclusions regarding the coupling efficiency of the process light with the feedstock material. However, it is possible to observe that a larger beam diameter (BS4 or BS6) requires an increase in terms of the energy delivered to the material. However, considering that a greater amount of material is being melted in these conditions, it is possible to expect that a constant specific energy is required to process the material. Hence, an analytical model that may help to explain such effects is the lumped heat capacity model.

B. Process feasibility with beam oscillation and in-source beam shaping

The second phase of the experimental investigation coupled the use of in-source shaping of the emission profile with dynamic oscillation of the laser beam. The process feasibility map with such techniques is reported in Fig. 8.

In this case, process feasibility conditions were determined for different beam shape combinations for $P = 600$ W. Lower levels of power resulted in no penetration joints, while over penetration was achieved when employing higher levels of power and lower scan velocities. Once again, it appears that a specific energy density controls the melting behavior of the material. Figure 9

shows the metallographic cross sections of the joints. Beam oscillation allows us to enlarge the seam width also in the case of welds performed with the Gaussian BS0 as shown in Fig. 9(a). However, in order to obtain a partial penetration, joint process productivity must be decreased with respect to linear welds for all beam shapes. However, the reduction in productivity when introducing beam oscillation is more contained in the case where the outer ring is employed.

Once again, by doubling the emission power from the BS0 condition ($P = 600$ W, $WA = 0.3$) to BS6 ($P = 1200$ W, $WA = 0.2$), it is possible to obtain partial penetration welds with the same process velocity ($v = 200$ mm/s). Hence, this indicates that at equal levels of power, a Gaussian beam is more efficient in performing a joint but this may be compensated by higher levels of emission power. On the other hand, lower peak irradiances are expected to generate less turbulent melt pools, which can reduce spatter formation.

The conditions selected for the comparison in terms of electromechanical properties are reported graphically in Fig. 8 and once again relate to the feasible combination of parameters capable of achieving partial penetration joints at a fixed level of emission power. Hence, in Table IV, the complete list of conditions selected for the comparison of the electromechanical properties of the joints is resumed.

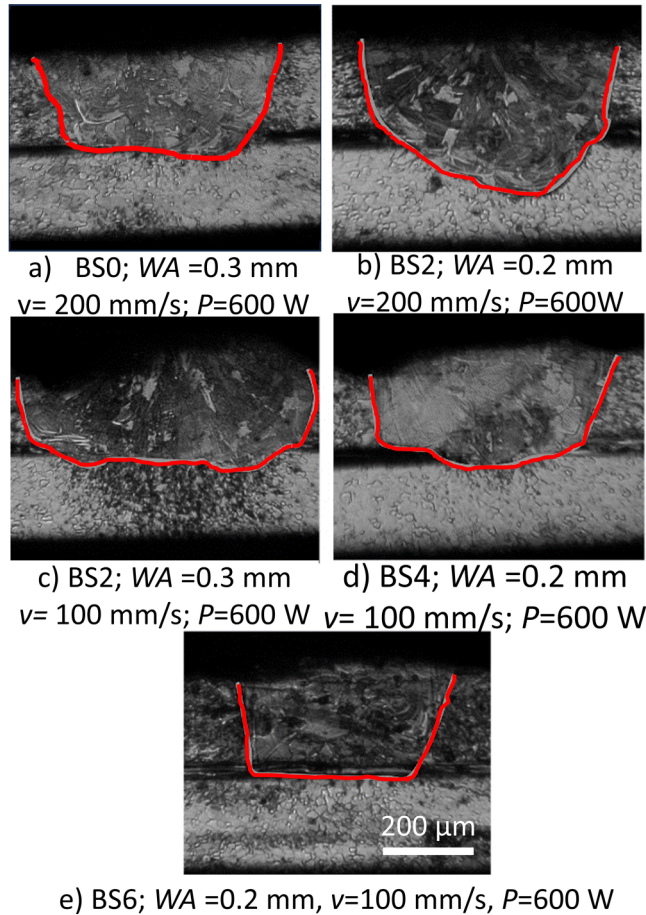


FIG. 9. Metallographic cross-sections of selected conditions with beam oscillation. Red line indicates melt profile.

C. Electrical and mechanical properties

Figure 10(a) reports the electrical resistance of the joints both for the single joint condition as well in iso-productivity situations where a greater number of weld lines was performed. In general, it is possible to observe that a single laser weld yields lower electrical resistance with respect to a connection performed by RSW. On the other hand, a double RSW joint allows us to achieve comparable results. Overall, it is possible to observe that non-significant differences appear between laser welded joints at a single joint level. The parameter that appears to affect most significantly the electrical resistance is the number of weld lines. However, given that larger weld seams obtained with doughnut beams or dynamic oscillation of the beam exhibit similar performance to narrow weld tracks performed with the gaussian beam shape, there is a strong indication that the most significant factor impacting over the electromechanical performance is the actual joint trajectory. This is in accordance with observations by Schmidt *et al.* who indicated that the weld geometry can have significant impacts on the performance of electrical connections.¹¹

TABLE IV. List of conditions selected to perform partial penetration welds on 0.2 + 0.2 mm Ni-plated steel lap joints. $p = 600$ W for all conditions.

Beam shaping	BS	WA (mm)	V (mm/s)
None	0	—	500
In-source	2	—	500
In-source	4	—	200
In-source	6	—	200
Wobbling	0	0.3	200
In-source + wobbling	2	0.2	200
In-source + wobbling	2	0.3	100
In-source + wobbling	4	0.2	100
In-source + wobbling	6	0.2	100

Figure 10(b) shows the UTF of the joints as a function of the different process conditions. It can be observed that the mechanical properties exhibit inverse trends with respect to the electrical resistance previously discussed.

Once again, the lower performance of RSW joints with respect to laser welded connections is confirmed. As mentioned in the Introduction, the main reason to support this technology resides on the lower chance of faults due to its higher resilience to gap formation during the welding process. In the case of linear welds, the different beam shaping techniques did not yield statistically significant different results. Only conditions with large wobble amplitudes ($WA = 0.3$ mm) possess higher mechanical resistance. However, once again the most significant factor results being the geometry of the weld trajectory obtained in the iso-productivity conditions where beam shapes with elevated levels of irradiance (BS0 and BS2) were employed to perform multiple adjacent weld tracks.

In Fig. 11, the mechanical strength and electrical resistance of the connections were correlated by a linear trend. A linear inverse relation can be observed indicating that a lower electrical resistance may be achieved when realizing connections with a higher mechanical strength. This result can be particularly appealing since it indicates that the mechanical strength of the battery pack cell to busbar joints may be certified by testing the electrical resistance in a non-destructive manner.

IV. DISCUSSION

Schmidt *et al.* indicated that electrical resistance is expected to be inversely correlated to the interface width.¹⁴ Hence, redistribution of the emission power to the outer core of the fiber was expected to yield joints with lower electrical resistance given the larger weld seams observable in Fig. 7. Analogously, the use of spatial beam oscillation has the capability of enlarging the width of the weld seam with respect to linear welds as demonstrated by the metallographic cross sections of Fig. 9. In the case of welding with dynamic beam oscillation, the use of different power density distributions is not reflected by changes in the geometry of the weld seam, as shown in Fig. 9, and the interface width measurements shown in Fig. 12. However, a correlation between the interface width and the electrical resistance could not be determined in the present investigation. This is in accordance with the results presented by Shaikh *et al.* during the welding of Cu-Hilumin where

17 October 2023 07:26:27

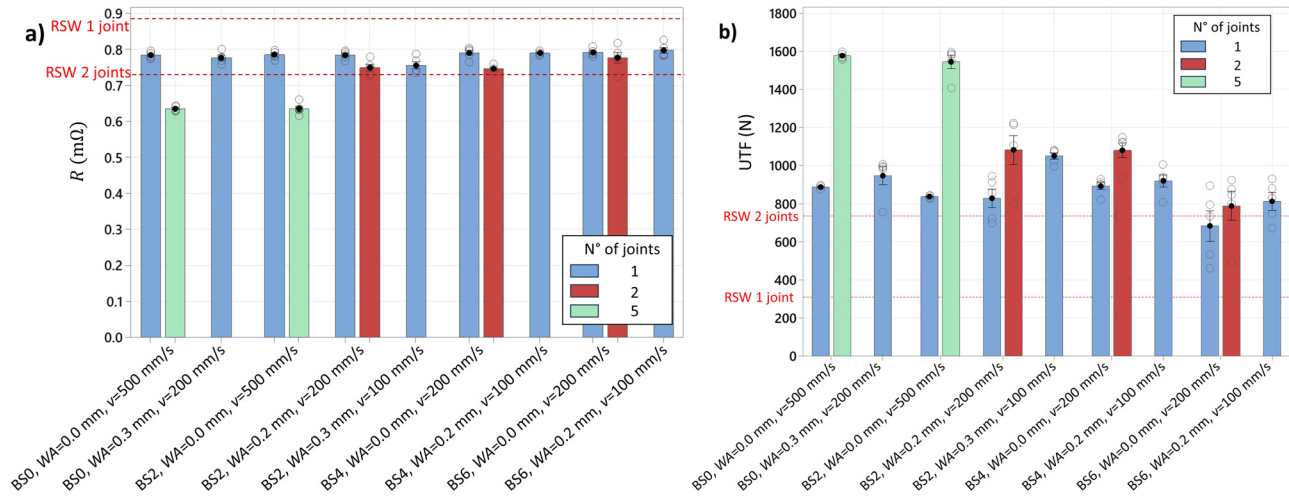


FIG. 10. (a) Electrical resistance and (b) UTF of the joints. WA = 0 indicates linear welds. Dashed red lines indicate electrical resistance of RSW joints. Error bars are one standard error from the mean.

non-significant differences in terms of electrical resistance were found at varying levels of interface width.²² Possibly this might be correlated to the fact that the superficial nickel plating is the main current carrying vector in Hilumin (given its higher conductivity with respect to steel). Hence, the flow of electrons can be expected to act mostly superficially. Further studies analyzing the material composition in the case of Hilumin–Hilumin joints may be required to disclose such effects, as well as comparative investigations with high current carrying materials such as Al and Cu with

tend to exhibit different behaviors as shown by Schmidt *et al.*¹⁴ Rather, the most significant factor resulted being the overall joint trajectory where multiple weld lines were capable of significantly reducing the overall electrical resistance as shown by the trend of Fig. 11. This can also be correlated with the increase in the contact

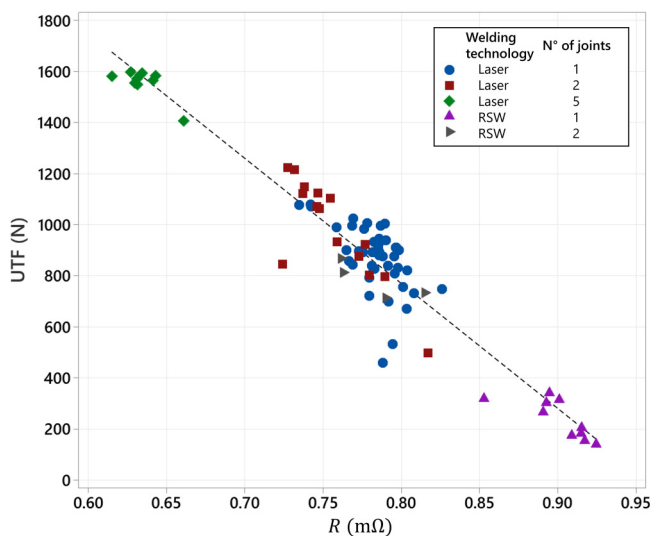


FIG. 11. UTF against electrical resistance R for the selected conditions categorized accordingly to the welding technology and the number of joints.

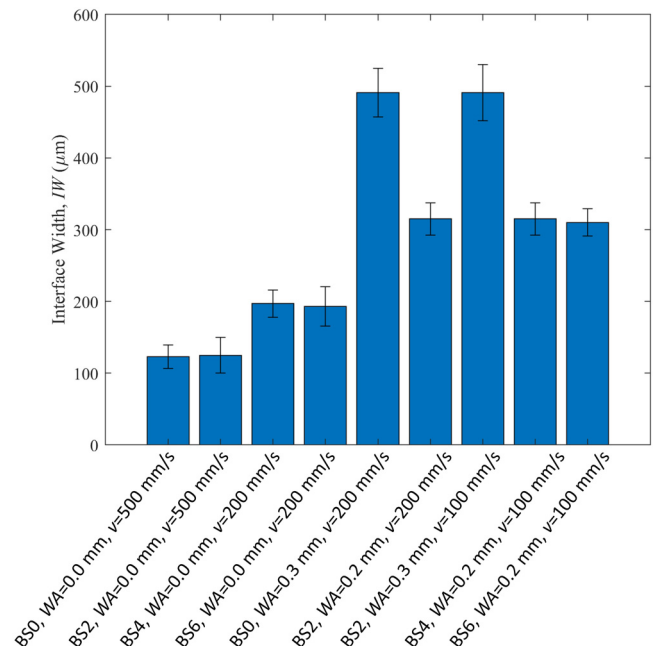


FIG. 12. Interface width of the selected joints. Error bars are 1 SD from the mean.

area between the two materials and also in-between the weld regions where effects similar to the mechanical locking mechanism may be expected.

In general, it must be considered that higher levels of irradiance allow us to achieve higher productivity. However, such effects can be easily compensated by the use of higher levels of emission power with doughnut-shaped beams. An aspect, which, however, has not been assessed in the present investigation, is the contamination of the weld region due to spatter formation. This is a fundamental point in the development of industrial laser based joining solution for the e-mobility sector, and it requires greater attention. Given that there is evidence that different beam shaping techniques may have an effect from this perspective, future works should also investigate these aspects.¹⁵

The overall results show that oscillation and in-source dynamic beam shaping techniques can provide a wide range of seam geometries adaptable to different application needs. A generic first allocation of the used techniques can be made considering the results. Gaussian beams can be employed to exploit higher process speed for thicker sections or where the full penetration does not generate an issue. The use of in-source beam shaping with ring beams can be exploited especially with cap to can and busbar to can connections, where limited penetration and a more stable keyhole are required. Wobbling can be exploited to potentially have a higher tolerance with gap formation. Future works will investigate the capacity of the beam shaping techniques to tolerate these defect types.

V. CONCLUSIONS

This investigation explored the use of in-source and dynamic beam oscillation as spatial beam shaping techniques during the laser welding of Ni-plated sheets for electric mobility applications representing typical cylindrical cell to busbar connections. The experimental investigations designed allowed us to determine process parameters for where successful partial penetration joints could be achieved. Finally, the selected conditions were characterized in terms of their electrical resistance and mechanical strength. Hence, it is possible to conclude that

- At equal levels of emission power, higher productivity could be obtained with beams with higher levels of irradiance. However, comparable productivity levels could be achieved by means of doughnut shaped beams by increasing the emission power, allowing the realization of connections with larger interface widths.
- The different beam shaping approaches did not yield statistically significant differences in terms of the electrical and mechanical properties at single joint level. On the other hand, the weld trajectory resulted being the most significant parameter.
- The mechanical resistance in terms of UTF is correlated by an inverse linear relationship to the electrical resistance.

Future developments of the present research will be aimed at disclosing the effects of the different beam shaping techniques on the process dynamics via high speed imaging. Moreover, there is interest in assessing the effects beam shaping techniques during the welding of dissimilar materials.

ACKNOWLEDGMENTS

Optoprim and nLIGHT are acknowledged for providing the laser source. The authors are thankful to Tata Steel for supplying the weld material and to Raylase for supporting the activities by providing the scanner head and controller card. The Italian Ministry of Education, University and Research is acknowledged for the support provided through the National Plan of Recovery and Resilience. The authors would like to thank Vittorio Maccone for the support in conducting the experimental activities.

AUTHOR DECLARATIONS

Conflict of Interest

The authors have no conflicts to disclose.

Author Contributions

Leonardo Caprio: Conceptualization (equal); Data curation (equal); Formal analysis (equal); Investigation (equal); Methodology (equal); Writing – original draft (equal); Writing – review & editing (equal). **Barbara Previtali:** Funding acquisition (equal); Project administration (equal); Resources (equal); Supervision (equal); Writing – review & editing (equal). **Ali Gökhan Demir:** Conceptualization (equal); Data curation (equal); Funding acquisition (equal); Methodology (equal); Project administration (equal); Supervision (equal); Writing – review & editing (equal).

REFERENCES

- ¹M. F. R. Zwicker, M. Moghadam, W. Zhang, and C. V. Nielsen, “Automotive battery pack manufacturing—A review of battery to Tab joining,” *J. Adv. Join Proc.* **1**, 100017 (2020).
- ²A. Das, D. Li, D. Williams, and D. Greenwood, “Joining technologies for automotive battery systems manufacturing,” *World Electr. Vehicle J.* **9**, 22 (2018).
- ³S. S. Lee, T. H. Kim, S. J. Hu, W. W. Cai, and J. A. Abell, “Joining technologies for automotive lithium-ion battery manufacturing: A review,” in *International Manufacturing Science and Engineering Conference*, Erie, Pennsylvania, October 12–15, 2010 (ASME, 2010), pp. 541–549.
- ⁴A. Kwade, W. Haselrieder, R. Leithoff, A. Modlinger, F. Dietrich, and K. Droeder, “Current status and challenges for automotive battery production technologies,” *Nat. Energy* **3**, 290–300 (2018).
- ⁵H. Löffberding, S. Wessel, C. Offermanns, M. Kehler, J. Rother, H. Heimes, and A. Kampker, “From cell to battery system in BEVs: Analysis of system packing efficiency and cell types,” *World Electr. Vehicle J.* **11**, 77–15 (2020).
- ⁶M. de Leon and H. S. Shin, “Review of the advancements in aluminum and copper ultrasonic welding in electric vehicles and superconductor applications,” *J. Mater. Process. Technol.* **307**, 117691 (2022).
- ⁷P. Taheri, S. Hsieh, and M. Bahrami, “Investigating electrical contact resistance losses in lithium-Ion battery assemblies for hybrid and electric vehicles,” *J. Power Sources* **196**, 6525–6533 (2011).
- ⁸C. Bolsinger, M. Zorn, and K. P. Birke, “Electrical contact resistance measurements of clamped battery cell connectors for cylindrical 18650 battery cells,” *J. Energy Storage* **12**, 29–36 (2017).
- ⁹N. Phichai, P. Kaewtatip, V. Lailuck, S. Rompho, and M. Masomtob, “Parametric effects of resistance spot welding between Li-ion cylindrical battery cell and nickel conductor strip,” in *IOP Conference Series: Materials Science and Engineering*, 11–14 December 2018 (Institute of Physics Publishing, Phuket, Thailand, 2019).

- ¹⁰J. Godek, "Joining lithium-ion batteries into packs using small-scale resistance spot welding," *Weld. Int.* **27**, 616–622 (2013).
- ¹¹M. J. Brand, P. A. Schmidt, M. F. Zaeh, and A. Jossen, "Welding techniques for battery cells and resulting electrical contact resistances," *J. Energy Storage* **1**, 7–14 (2015).
- ¹²M. S. Zediker, R. D. Fritz, M. J. Finuf, and J. M. Pelaprat, "Laser welding components for electric vehicles with a high-power blue laser system," *J. Laser Appl.* **32**, 022038 (2020).
- ¹³S. Grabmann, J. Kriegler, F. Harst, F. J. Günter, and M. F. Zaeh, "Laser welding of current collector foil stacks in battery production—mechanical properties of joints welded with a green high-power disk laser," *Int. J. Adv. Manuf. Technol.* **118**, 2571–2586 (2022).
- ¹⁴P. A. Schmidt, M. Schweizer, and M. F. Zaeh, "Joining of lithium-ion batteries using laser beam welding: Electrical losses of welded aluminum and copper joints," in *ICALEO 2012—31st International Congress on Applications of Lasers and Electro-Optics* (Laser Institute of America, 2012), Vol. 915, pp. 915–923.
- ¹⁵E. Punzel, F. Hugger, T. Dinkelbach, and A. Bürger, "Influence of power distribution on weld seam quality and geometry in laser beam welding of aluminum alloys," *Procedia CIRP*, 601–604 (2020).
- ¹⁶C. Prieto, E. Vaamonde, D. Diego-Vallejo, J. Jimenez, B. Urbach, Y. Vidne, and E. Shekel, "Dynamic laser beam shaping for laser aluminium welding in E-mobility applications," *Procedia CIRP*, 596–600 (2020).
- ¹⁷T. Sun, P. Franciosa, M. Sokolov, and D. Ceglarek, "Challenges and opportunities in laser welding of 6xxx high strength aluminium extrusions in automotive battery tray construction," *Procedia CIRP* **94**, 565–570 (2020).
- ¹⁸G. Chianese, S. Jabar, P. Franciosa, D. Ceglarek, and S. Patalano, "A multi-physics CFD study on the part-to-part Gap during remote laser welding of copper-to-steel battery Tab connectors with beam wobbling," *Procedia CIRP*, 484–489 (2022).
- ¹⁹J. S. Rinne, S. Nothdurft, J. Hermsdorf, S. Kaierle, and L. Overmeyer, "Advantages of adjustable intensity profiles for laser beam welding of steel copper dissimilar joints," *Procedia CIRP* **94**, 661–665 (2020).
- ²⁰T. Sun, A. Mohan, C. Liu, P. Franciosa, and D. Ceglarek, "The impact of adjustable-ring-mode (ARM) laser beam on the microstructure and mechanical performance in remote laser welding of high strength aluminium alloys," *J. Mater. Res. Technol.* **21**, 2247–2261 (2022).
- ²¹F. Galbusera, L. Caprio, B. Previtali, and A. G. Demir, "The influence of novel beam shapes on melt pool shape and mechanical properties of LPBF produced Al-alloy," *J. Manuf. Process* **85**, 1024–1036 (2023).
- ²²U. F. Shaikh, A. Das, A. Barai, and I. Masters, "Electro-thermo-mechanical behaviours of laser joints for electric vehicle battery interconnects," in *2019 Electric Vehicles International Conference (EV), Bucharest, Romania, 3–4 October 2019* (IEEE, 2019), pp. 1–6.